11-2009

Coupled Ray-Tracing and Fokker-Planck EBW Modeling for Spherical Tokamaks

Jakub Urban

Joan Decker

Y. Peysson

Josef Preinhaelter

Gary Taylor

See next page for additional authors

Original Publication Citation

Urban, J., Decker, J., Peysson, Y., Preinhaelter, J., Taylor, G., Vahala, L., & Vahala, G. (2009). *Coupled ray-tracing and Fokker-Planck EBW modeling for spherical tokamaks.* Paper presented at the Radio Frequency Power in Plasmas, 24-26 June 2009, USA. http://dx.doi.org/10.1063/1.3273793

Coupled Ray-tracing and Fokker-Planck EBW Modeling for Spherical Tokamaks

J. Urban,[a] J. Decker,[b] Y. Peysson,[b] J. Preinhaelter,[a] G. Taylor,[c] L. Vahala,[d] G. Vahala[e]

[a] *EURATOM/IPP.CR Association, 182 00 Prague, Czech Republic*
[b] *EURATOM-CEA, Cadarache, France*
[c] *Princeton Plasma Physics Laboratory, Princeton, NJ 08543, USA*
[d] *Old Dominion University, Norfolk, VA 23529, USA*
[e] *College of William & Mary, Williamsburg, VA 23185, USA*

Abstract. The AMR (Antenna—Mode-conversion—Ray-tracing) code [1, 2] has been recently coupled with the LUKE [3] Fokker-Planck code. This modeling suite is capable of complex simulations of electron Bernstein wave (EBW) emission, heating and current drive. We employ these codes to study EBW heating and current drive performance under spherical tokamak (ST) configurations—typical NSTX discharges are employed. EBW parameters, such as frequency, antenna position and direction, are varied and optimized for particular configurations and objectives. In this way, we show the versatility of EBWs.

Keywords: Fusion, tokamak, heating, current drive, electron Bernstein wave, EBW.
PACS: 52.35.Hr, 52.50.Sw, 52.55.Fa.

INTRODUCTION

While the "standard" electron cyclotron heating and current drive (ECH/ECCD) are among the most important auxiliary systems for present and future magnetic fusion devices, their application to spherical tokamaks, which operate in "overdense" regimes (i.e., the electron plasma frequency ω_{pe} is much greater than the electron cyclotron frequency ω_{ce}), is generally impossible because the involved ordinary (O) and extraordinary (X) electron cyclotron waves are cutoff in the fundamental electron cyclotron (EC) harmonics range. Using higher harmonics is not possible because of poor absorption. The only possibility are the electron Bernstein waves [4] (EBWs)—electrostatic electron cyclotron waves, which can propagate in overdense plasmas. EBWs are typically very well absorbed at any EC harmonic and they can efficiently drive current because of their interaction with supra-thermal electrons. The drawback of EBWs is the fact that they must be excited by O- or X-modes via a mode conversion process. The waves must be injected under specific angles to achieve an efficient conversion. EBWs are also more difficult to control—they are tightly coupled with the plasma parameters, particularly the magnetic field and the electron density and temperature profiles.

In this paper, we present a survey of EBW heating and current drive possibilities for spherical tokamaks. The study has been performed with two coupled simulation codes—AMR [1, 2], which provides mode conversion and ray-tracing calculations, and LUKE [3], a Fokker-Planck code, which provides quasi-linear power deposition and current drive calculations. Various injection scenarios are considered for typical NSTX conditions.

CP1187, *Radio Frequency Power in Plasmas*
edited by V. Bobkov and J.-M. Noterdaeme

SIMULATION METHODS

A Gaussian antenna beam is assumed in the simulation, with the beam waist close to the target plasma and with a fixed Rayleigh range to obtain a realistic waist size with a reasonable divergence. The toroidal and poloidal launch angles θ_{tor} and θ_{pol} are always chosen optimum for the O-X-B conversion process. The mode conversion efficiency is calculated by the AMR code. The O-X-B scenario is preferred because it can be used at any frequency and density gradient, which is not the case of the direct X-B conversion.

Electron Bernstein wave propagation is well described by standard ray-tracing with the non-relativistic hot-plasma electrostatic dispersion relation (see, e.g., [5, 6]). The imaginary part of the dispersion relation determines the wave packet damping along the ray trajectory [7]:

$$\frac{\mathrm{d}P}{\mathrm{d}t} = -\alpha P = \frac{2\,\mathrm{Im}\,D}{\left|\partial\,\mathrm{Re}\,D/\partial\omega\right|} P. \tag{1}$$

For the wave damping in fusion-relevant plasmas, however, a relativistic correction to α is necessary [8]. We have included a simple (weakly) relativistic damping rate into the AMR ray-tracing (eq. (39) from [8]), which accounts for the relativistic shift of the resonance:

$$\mathrm{Im}\,D^{(\mathrm{relativistic})} = \frac{\sqrt{\pi}\omega}{\left|k_{\parallel}\right| v_T} \frac{\omega_{\mathrm{pe}}^2}{\omega_{\mathrm{ce}}^2} \sum_n \frac{I_n(b) e^{-b}}{b} e^{-p_n^2}, \tag{2}$$

where

$$p_n \equiv p_{n0}\left(1 + \left|\frac{p_{n0}}{2N_{\parallel}}\right| \frac{v_{\mathrm{T}}}{c}\right),\ p_{n0} \equiv \frac{\omega - n\omega_{\mathrm{ce}}}{k_{\parallel} v_{\mathrm{T}}},\ v_{\mathrm{T}} \equiv \left(\frac{2\kappa T_{\mathrm{e}}}{m_{\mathrm{e}}}\right)^{1/2},\ b \equiv \frac{k_{\perp}^2 v_{\mathrm{T}}^2}{2\omega_{\mathrm{ce}}^2}. \tag{3}$$

Ray-tracing results, particularly the ray trajectories with the $N_{\parallel}$ and $N_{\perp}$ wave vector components evolution, provide the input for the LUKE 3D (p, $p_{\parallel}/p$, ψ) Fokker-Planck code, which then calculates the quasilinear wave damping and current drive. The equilibrium and plasma profiles are identical in AMR and LUKE.

RESULTS

Shown here are AMR + LUKE simulation results for a typical NSTX L-mode. Results for an H-mode are not completely available and have not been analyzed yet. First and second harmonic ranges 12 – 18 GHz and 22 – 28 GHz have been chosen because of their estimative accessibility. Higher harmonics would also be possible, however, with a risk of harmonic overlapping, which would decrease the current drive efficiency. A Gaussian antenna beam with the Rayleigh range of 0.5 m, focused almost to the last closed flux surface (LCFS), is assumed, with power $P = 1\,\mathrm{MW}$.

First, the optimum antenna angles (toroidal and poloidal) are calculated by AMR. In Fig. 1 are shown the angular windows for the first and the second harmonic ranges in two different vertical antenna positions. The angular windows are quite broad, which makes the antenna aiming less sensitive to misalignments. The large angular width is due to the relatively steep density gradient. The H-mode gradient is even steeper, enabling efficient conversion at a very broad range of angles. The optimum angles are, however, different in L- and H-mode because of different poloidal magnetic field.

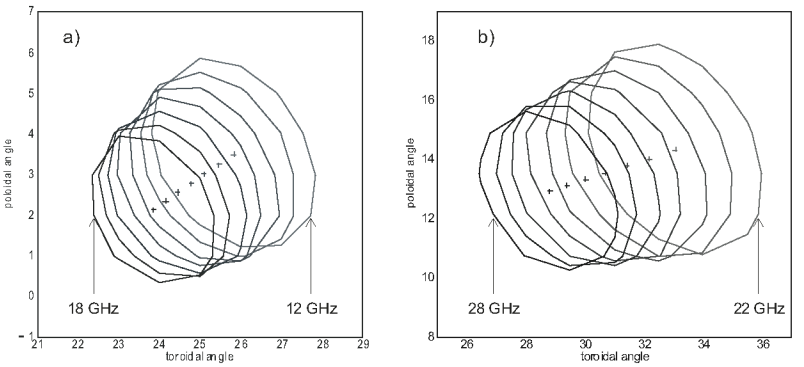

FIGURE 1. Angular O-X-EBW windows for a) first harmonic range 12 – 18 GHz, mid-plane launch, b) second harmonic range 22 – 28 GHz, Z=0.2 m launch. Contours show 90 % conversion efficiency, cross-marks the optimum angles for each frequency. NSTX L-mode parameters.

Two EBW launching parameters can be chosen arbitrarily—the frequency and the vertical antenna position Z_A. Two (opposite) toroidal angles are then possible for given frequency and antenna position. It is well known, and validated by our ray-tracing results, that EBWs rays (and their $N_\parallel$) typically oscillate when launched close to the mid-plane. $|N_\parallel|$ can become very small (<0.1) in such cases, which minimizes the Doppler shift and thus the waves are absorbed in a close vicinity of the EC resonance $\omega - n\omega_{ce}$. The damping location of the mid-plane EBWs can therefore be easily determined. Such scenario can be favorable for central heating, but is very unfavorable for current drive because of the small $N_\parallel$ with a random sign.

The ray-tracing/Fokker-Planck results for the NSTX L-mode are shown in Fig. 2. This figure demonstrates the dependence of the deposition location ρ^{max} and the total driven current on the two main parameters—the frequency and the vertical antenna position. The current drive efficiency $\zeta \cong 3.27 I R_0 n_e / P T_e$ [9] is also calculated. The accessibility in these cases is approximately $0.1 < \rho < 0.6$ for the first harmonic and $0.2 < \rho < 0.8$ for the second harmonic waves. The current direction is determined by the $N_\parallel$ sign and by the current drive mechanism—Fisch-Boozer or Ohkawa. The toroidal launch angle (not shown here) plays a role only if the deposition takes place at the edge; otherwise, the $N_\parallel$ sign is determined by Z_A only. Fisch-Boozer is the dominant mechanism at smaller radii, while Ohkawa current drive becomes important closer to the edge, where the trapped particles fraction increases. These two mechanisms can cancel and consequently no net current is driven in certain cases. In most cases, the current drive is more efficient at the first harmonic.

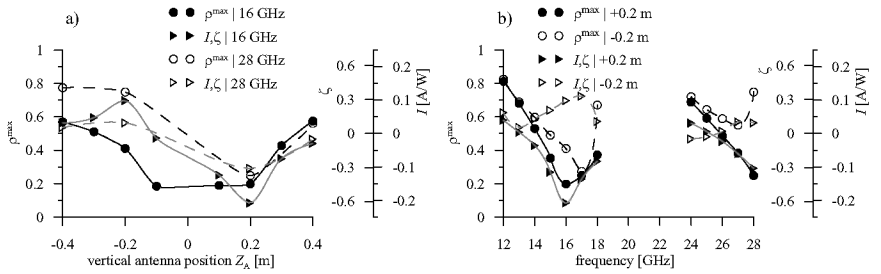

FIGURE 2. Deposition location ρ^{max} and the total driven current I versus a) vertical antenna position Z_A for 16 GHz, b) frequency for $Z_A = \pm 0.2$ m.

CONCLUSIONS AND OUTLOOK

The O-X-EBW coupling is efficient in broad angular windows around the optimum angles, which depend on Z_A, frequency, and the plasma parameters. The excited EBWs can efficiently be absorbed and drive current at certain radii. The current direction is determined by Z_A (above / below the mid-plane). The deposition location can be controlled by changing either Z_A or the frequency. The frequency-based control provides larger radial range and the ρ^{max} dependence is clearer and smoother. This method would, however, require technologically challenging step-tunable gyrotrons. Changing Z_A, on the other hand, requires complex antenna and adjusting the angles at each vertical position.

More simulations will be performed and analyzed, particularly for the NSTX H-mode, and also for other present and future devices (e.g., MAST and MAST-Upgrade). This will bring a better insight into EBWs' capabilities.

ACKNOWLEDGMENTS

The work was partly supported by EFDA Fusion Researcher Fellowship, by the grant no. 202/08/0419 of Czech Science Foundation, by U.S. Department of Energy, by EURATOM and by the Academy of Sciences of the Czech Republic.

REFERENCES

1. J. Urban, and J. Preinhaelter, *J. Plas. Phys.* **72**, 1041 (2006).
2. J. Urban et al., in *ICCP 2008*, Fukuoka, Japan. To be published in *Journal of Plasma and Fusion Research Series*.
3. J. Decker, and Y. Peysson, *DKE: a fast numerical solver for the 3-D relativistic bounce-averaged electron drift kinetic equation*, EURATOM-CEA report EUR-CEA-FC-1736, 2004.
4. I. B. Bernstein, *Physical Review* **109**, 10 (1958).
5. V. L. Ginzburg, and A. A. Rukhadze, *Volny v magnitoaktivnoi plazme,* Nauka: Moskva, 1975.
6. T. H. Stix, *Waves in plasmas,* American Institute of Physics: New York, 1992.
7. P. T. Bonoli, and R. C. Englade, *Physics of Fluids* **29**, 2937 (1986).
8. J. Decker, and A. K. Ram, *Phys. Plas.* **13**, 112503 (2006).
9. C. C. Petty et al., *Nuclear Fusion* **42**, 1366 (2002).